

Structural Investigations of Palladium(II) and Platinum(II) Complexes of Salicylhydroxamic Acid

Matthew D. Hall, Timothy W. Failes, David E. Hibbs, and Trevor W. Hambley*

Centre for Heavy Metals Research, School of Chemistry, The University of Sydney, New South Wales 2006, Australia

Received July 17, 2001

Complexes of salicylhydroxamic acid (shaH) with palladium(II) and platinum(II) were investigated. The synthesis of $[\text{Pt}(\text{sha})_2]$ was attempted via a number of methods, and ultimately ^1H NMR investigations revealed that salicylhydroxamate would not coordinate to chloro complexes of platinum(II). However, $[\text{Pt}(\text{sha}-\text{H})(\text{PPh}_3)_2]$ was successfully synthesized and the crystal structure determined (orthorhombic, space group $Pca2_1$, $a = 17.9325(19)$ Å, $b = 11.3102(12)$ Å, $c = 18.2829(19)$ Å, $Z = 4$, $R = 0.0224$). The sha binds via an $[O,O]$ binding mode, in its hydroxamate form. In contrast the palladium complex $[\text{Pd}(\text{sha})_2]$ was readily synthesized and crystallized as $[\text{Pd}(\text{sha})_2](\text{DMF})_4$ in the triclinic space group $P\bar{1}$, $a = 7.066(1)$ Å, $b = 9.842(2)$ Å, $c = 12.385(2)$ Å, $\alpha = 99.213(3)^\circ$, $\beta = 90.669(3)^\circ$, $\gamma = 109.767(3)^\circ$, $Z = 1$, $R = 0.037$. The unexpected $[\text{N},\text{O}']$ binding mode of the salicylhydroxamate ligand in $[\text{Pd}(\text{sha})_2]$ prompted investigation of the stability of a number of binding modes of salicylhydroxamic acid in $[\text{M}(\text{sha})_2]$ ($\text{M} = \text{Pd}, \text{Pt}$) by density functional theory, using the B3LYP hybrid functional at the 6-311G* level of theory. Geometry optimizations were carried out for various binding modes of the ligands and their relative energies established. It was found that the $[\text{N},\text{O}']$ mode gave the more stable complex, in accord with experimental observations. Stabilization of hydroxamate binding to platinum is evidently afforded by soft ligands lying trans to them.

Introduction

Hydroxamic acids are involved in numerous biological processes including metal ion transport and inhibition of metalloproteins such as matrix metalloproteinases (MMPs) and ureases. MMPs have a natural role in tissue remodeling, but have also been implicated in a number of disease states including multiple sclerosis, rheumatoid arthritis, and tumor metastasis.^{1–3}

The catalytic site of MMPs contains a zinc(II) ion which binds to and facilitates the hydrolysis of peptides in basement membranes.⁴ Tissue inhibitors of metalloproteinases (TIMPs) possess a hydroxamic acid moiety which binds in a bidentate fashion via two oxygen donor atoms to the zinc(II) of the MMP active site,^{5–7} and a number of MMP inhibitors based on the hydroxamic acid group have been synthesized and

have entered clinical trials (e.g., batimastat and marimastat).⁸ Urease is a dinickel enzyme that catalyzes the hydrolysis of urea within microbial nitrogen metabolism,^{9,10} and is inhibited by hydroxamates.⁹ It has been shown crystallographically to coordinate both Ni(II) ions.^{11,12} The hydroxamate functional group is also present in siderophores, naturally occurring trihydroxamate compounds that sequester and

* To whom correspondence should be addressed. Phone: 61-2-9351-2830. Fax: 61-2-9351-3329. E-mail: t.hambley@chem.usyd.edu.au.

- (1) Michaelides, M. R.; Curtin, M. L. *Curr. Pharm. Des.* **1999**, *5*, 787–819.
- (2) Borkakoti, N. *Prog. Biophys. Mol. Biol.* **1998**, *70*, 73–94.
- (3) Johansson, N.; Ahonen, M.; Kahari, V.-M. *Cell. Mol. Life Sci.* **2000**, *57*, 5–15.
- (4) Auld, D. S. *Struct. Bonding (Berlin)* **1997**, *89*, 29–50.

- (5) Betz, M.; Huxley, P.; Davies, S. J.; Mushtaq, Y.; Pieper, M.; Tschesche, H.; Bode, W.; Gomis-Ruth, F. X. *Eur. J. Biochem.* **1997**, *247*, 356–363.
- (6) Dhanaraj, V.; Williams, M. G.; Ye, Q.-Z.; Molina, F.; Johnson, L. L.; Ortwine, D. F.; Pavlovsky, A.; Rubin, J. R.; Skeeane, R. J.; Skeeane, R. W.; White, A. D.; Humblet, C.; Hupe, D. J.; Blundell, T. L. *Croat. Chem. Acta* **1999**, *72*, 575–591.
- (7) Dhanaraj, V.; Ye, Q.-Z.; Johnson, L. L.; Hupe, D. J.; Ortwine, D. F.; Dunbar, J. B., Jr.; Rubin, J. R.; Pavlovsky, A.; Humblet, C.; Blundell, T. L. *Structure* **1996**, *4*, 375–386.
- (8) Cawston, T. E. *Pharmacol. Ther.* **1996**, *70*, 163–182.
- (9) Ciurli, S.; Benini, S.; Rypniewski, W. R.; Wilson, K. S.; Miletta, S.; Mangani, S. *Coord. Chem. Rev.* **1999**, *190–192*, 331–355.
- (10) Ermler, U.; Grabarse, W.; Shima, S.; Goubeaud, M.; Thauer, R. K. *Curr. Opin. Struct. Biol.* **1998**, *8*, 749–758.
- (11) Benini, S.; Rypniewski, W. R.; Wilson, K. S.; Miletta, S.; Ciurli, S.; Mangani, S. *J. Biol. Inorg. Chem.* **2000**, *5*, 110–118.
- (12) Pearson, M. A.; Michel, L. O.; Hausinger, R. P.; Karplus, P. A. *Biochemistry* **1997**, *36*, 8164–8172.

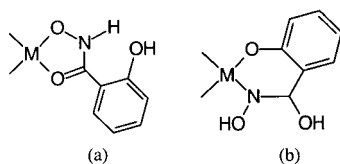


Figure 1. Two possible binding modes for salicylhydroxamic acid: (a) $[O,O]$ and (b) $[N,O']$.

solubilize iron. Microbial iron acquisition is then facilitated by active uptake of the bound iron–siderophore complex.¹³ On the basis of this feature, a range of compounds containing hydroxamic acids have been synthesized and tried as iron chelators for the treatment of iron overload diseases (e.g., thalassemia), though at present the only iron chelator in clinical use is desferrioxamine.¹⁴

Given the prevalence of the hydroxamate moiety in biological systems, we were interested in the effect (if any) that platinum-based anticancer drugs would have on this functional group in vivo and whether they could be used as carriers of the platinum drugs. Hydroxamic acids were first isolated in 1869, and their structure and chemistry have been developed and reviewed extensively.^{15–17} In addition to the role hydroxamic acids play in organic synthesis, many transition-metal complexes have been synthesized. Hydroxamates can form stable metal complexes through the two oxygen atoms of the hydroxamate functional group with transition-metal ions that are hard (HSAB).^{18,19} Of particular initial interest in this instance, however, are complexes with the softer (HSAB) platinum metals; some were reported by Mishra, who described complexes with Ru(III), Rh(III), Pd(II), and Ir(II) but not Pt(II).^{20,21} Salicylhydroxamate (sha^-) can chelate via a number of possible coordination modes, not only the $[O,O]$ mode as shown in Figure 1a, but also $[N,O']$ with the phenolato oxygen as the O -donor, shown in Figure 1b. While in most instances the hydroxamates are bound via the $[O,O]$ chelating mode, other coordination modes have also been reported, though none in the same fashion as that shown in Figure 1b.

In this study, complexes of salicylhydroxamate with palladium(II) and platinum(II) were investigated, and the relative stabilities of the binding modes shown in Figure 1 for $[\text{M}(\text{sha})_2]$ ($\text{M} = \text{Pd}, \text{Pt}$) were investigated by molecular orbital methods. The use of density functional theory (DFT) calculations provides valuable insight into the properties of metal complexes that are difficult to obtain synthetically, and has previously been used to determine the proportion of coordination isomers of aminohydroxamate molybdenum complexes in solution.²²

Experimental Section

Instrumentation and Materials. ^1H NMR spectra were recorded at 298 K on a Bruker AMX 400 MHz spectrometer. All spectra were recorded using commercially available D_2O (Aldrich) of 99.6% isotopic purity or better and referenced to solvent impurities. X-ray crystallographic data were collected on a Bruker-AXS SMART 1000 CCD system and analyzed using SAINT²³ and teXsan²⁴ software. The ORTEP program was used to produce the drawings.²⁵ Elemental analysis (C, H, N) was conducted by the Microanalytical Service of the Australian National University. $\text{K}_2[\text{PdCl}_4]$ and shaH were obtained from Aldrich, $\text{K}_2[\text{PtCl}_4]$ was obtained from Aithaca Chemical Corp., and all three were used without further purification. *cis*- $[\text{PtCl}_2(\text{PPh}_3)_2]$ was prepared as previously described.²⁶

Synthesis of Bissalicylhydroxamatopalladium(II), $[\text{Pd}(\text{sha})_2]$. $\text{K}_2[\text{PdCl}_4]$ (0.10 g, 3.1×10^{-4} mol) was dissolved in water (5 mL), and a 3-fold excess of salicylhydroxamic acid (shaH) (0.15 g, 9.2×10^{-4} mol) was added. This solution was stirred at 50 °C for 2 h, during which time a copious amount of product precipitated. The light yellow solid was collected, washed with cold water, recrystallized from acetone, and dried in a desiccator, yielding $[\text{Pd}(\text{sha})_2]$ (0.093 g, 2.3×10^{-4} mol, 73% based on Pd). IR (KBr, cm^{-1}): 3411 vs, 3376 s, 3100 br, 1672 vs, 1600 s, 1548 m, 1468 vs, 1435 m, 1393 s, 1332 vs, 1201 s, 1158 m, 1144 m, 1085 m, 1045 w, 1032 s, 893 vs, 844 m, 765 m, 758 m, 742 m, 691 w, 666 s, 594 w, 536 m, 489 w, 446 w. Anal. Calcd: C, 40.95; H, 2.95; N, 6.82. Found: C, 40.34; H, 2.86; N, 7.09. Good-quality crystals of $[\text{Pd}(\text{sha})_2] \cdot 4\text{DMF}$ were obtained from a cooled, saturated DMF solution for crystallographic studies.

Synthesis of Salicylhydroxamatobis(triphenylphosphine)-platinum(II), $[\text{Pt}(\text{sha-H})(\text{PPh}_3)_2]$. To a suspension of *cis*- $[\text{PtCl}_2(\text{PPh}_3)_2]$ (0.10 g, 0.13 mmol) in methanol (10 mL) was added salicylhydroxamic acid (0.019 g, 0.13 mmol). Aqueous NaOH (1M) was added dropwise with stirring to the reaction mixture until the pH reached 10, whereupon the starting materials gradually dissolved and a yellow precipitate formed rapidly. The product was collected, washed with a little cold methanol and ether, and air-dried, yielding $[\text{Pt}(\text{sha-H})(\text{PPh}_3)_2]$ (0.069 g, 0.078 mmol, 63% based on Pt). IR (KBr, cm^{-1}): 3053 w, 1595 m, 1554 w, 1494 m, 1482 m, 1437 m, 1344 m, 1303 m, 1267 m, 1235 w, 1127 w, 1095 m, 1080 w, 999 w, 926 w, 835 w, 769 w, 746 s, 706 s, 692 vs, 618 m, 570 m, 554 vs, 530 vs, 512 s, 505 s, 420 s. Anal. Calcd: C, 59.31; H, 4.05; N, 1.61. Found: C, 59.21; H, 4.37; N, 1.78. Good-quality crystals of $[\text{Pt}(\text{sha-H})(\text{PPh}_3)_2]$ were obtained by diffusion of ethanol into a DMF solution of the product.

X-ray Crystallography. The crystals chosen for data collection were attached to thin glass fibers and mounted onto a Bruker SMART 1000 CCD diffractometer employing graphite-monochromated Mo $\text{K}\alpha$ radiation generated from a sealed tube. The intensities of 50 standard reflections recollected at the end of the experiments did not change significantly during the data collections. Empirical absorption corrections determined with SADABS²⁷ were applied to the data, and the data integration and reduction were undertaken with SAINT and XPREP.²³ The data reduction included the

(13) Roosenberg, J. M.; Lin, Y. M.; Lu, Y.; Miller, M. J. *Curr. Med. Chem.* **2000**, *7*, 159–197.

(14) Richardson, D. R.; Ponka, P. *J. Lab. Clin. Med.* **1998**, *131*, 306–315.

(15) Lossen, H. *Ann. Chem. Pharm.* **1869**, *150*, 314–322.

(16) Bauer, L.; Exner, O. *Angew. Chem., Int. Ed. Engl.* **1974**, *13*, 376–384.

(17) Yale, H. L. *Chem. Rev.* **1943**, *33*, 209–256.

(18) Chatterjee, B. *Coord. Chem. Rev.* **1978**, *26*, 281–303.

(19) Kurzak, B.; Kozłowski, H.; Farkas, E. *Coord. Chem. Rev.* **1992**, *114*, 169–200.

(20) Mishra, R. S. *J. Indian Chem. Soc.* **1967**, *44*, 400.

(21) Mishra, R. S. *J. Indian Chem. Soc.* **1969**, *46*, 1074–1077.

(22) Farkas, E.; Csoka, H.; Bell, G.; Brown, D. A.; Cuffe, L. P.; Fitzpatrick, N. J.; Glass, W. K.; Errington, W.; Kemp, T. J. *J. Chem. Soc., Dalton Trans.* **1999**, 2789–2794.

(23) Bruker Analytical X-ray Instruments Inc., Madison, WI, 1995.

(24) Molecular Structure Corp., 3200 Research Forest Dr., The Woodlands, TX, 77381, 1997–1998.

(25) Johnson, C. K., Oak Ridge National Laboratory, Oak Ridge, TN, 1976.

(26) Bailar, J. C., Jr.; Itatani, H. *Inorg. Chem.* **1965**, *4*, 1618–1620.

(27) Sheldrick, G. M., University of Göttingen, Germany, 1996.

Table 1. Crystal Data and Structure Refinement for [Pd(sha)₂]₂·4DMF and [Pt(sha)(PPh₃)₂]

	[Pd(sha) ₂] ₂ ·4DMF	[Pt(sha)(PPh ₃) ₂]
empirical formula	PdC ₂₆ H ₄₀ N ₆ O ₁₀	PtC ₄₃ H ₃₅ NO ₃ P ₂
fw	703.04	870.75
space group	<i>P1</i>	<i>Pca2</i> ₁
<i>a</i> , Å	7.066(1)	17.9325(19)
<i>b</i> , Å	9.842(2)	11.3102(12)
<i>c</i> , Å	12.385(2)	18.2829(19)
α, deg	99.213(3)	90
β, deg	90.669(3)	90
γ, deg	109.767(3)	90
<i>V</i> , Å ³	798.1(2)	3708.1(7)
<i>Z</i>	1	4
μ, mm ⁻¹	0.643	3.911
ρ _{obsd} , g cm ⁻³	1.463	1.560
<i>T</i> , K	293	293
λ, Å	0.71073	0.71073
<i>R</i> (<i>F</i> _o) ^a	0.037	0.022
<i>R</i> _w ^a	0.034	0.059

$$^a R(F_o) = \sum ||F_o| - |F_c|| / \sum |F_o|. R_w = (\sum w(|F_o| - |F_c|)^2 / \sum w|F_o|^2)^{1/2}, w = 1/\sigma^2(F_o).$$

application of Lorentz and polarization corrections. The structures were solved by direct methods with SHELXS-86,²⁸ and extended and refined using teXsan.²⁴ The structures were refined on *F*² by full-matrix least-squares with anisotropic thermal parameters for all non-H atoms and calculated (riding model) positions for H atoms with *U*_{ij} set at 1.5 times that of the parent atom. Final *R* indices and weighting schemes are as quoted in Table 1.

¹H NMR Solution Study. K₂[PtCl₄] (0.076 g, 1.6 × 10⁻⁴ mol) was dissolved in D₂O (10 mL), and two stoichiometric equivalents of shaH (0.050 g, 3.3 × 10⁻⁴ mol) were added to the solution. Three aliquots of the reaction mixture were adjusted to pH values of 2, 5, and 13 using DCl and NaOD. Following equilibration for 4 h at 37 °C, ¹H NMR spectra were collected for each of the three solutions. The solutions were retained and protected from light at 37 °C, and the ¹H NMR spectra were collected again after 7 and 14 days where decomposition had not occurred.

Computational Details. Calculations were carried out using the Gaussian 98²⁹ program package running on a Silicon Graphics workstation. Molecular orbital calculations were carried out using density functional theory (B3LYP)^{30–32} methods. These used the Stuttgart effective core potential SDD³³ for the metal atoms. SDD contains a scalar relativistic pseudopotential for the core electrons and a [6s,5p,3d] contracted Gaussian basis for valence electrons. The remaining atoms were assigned the Dunning/Hazinaga³⁴ double-ζ valence basis set. During the geometry optimizations the complexes were constrained to have C_s symmetry.

(28) Sheldrick, G. M., University of Göttingen, Germany, 1986.

(29) Frisch, M. J.; Trucks, G. W.; Schlegel, H. B.; Scuseria, G. E.; Robb, M. A.; Cheeseman, J. R.; Zakrzewski, V. G.; Montgomery, J., J. A.; Stratmann, R. E.; Burant, J. C.; Dapprich, S.; Millam, J. M.; Daniels, A. D.; Kudin, K. N.; Strain, M. C.; Farkas, O.; Tomasi, J.; Barone, V.; Cossi, M.; Cammi, R.; Mennucci, B.; Pomelli, C.; Adamo, C.; Clifford, S.; Ochterski, J.; Petersson, G. A.; Ayala, P. Y.; Cui, Q.; Morokuma, K.; Malick, D. K.; Rabuck, A. D.; Raghavachari, K.; Foresman, J. B.; Cioslowski, J.; Ortiz, J. V.; Baboul, A. B.; Stefanov, B. B.; Liu, G.; Liashenko, A.; Piskorz, P.; Komaromi, I.; Gomperts, R.; Martin, R. L.; Fox, D. J.; Keith, T.; Al-Laham, M. A.; Peng, C. Y.; Nanayakkara, A.; Gonzalez, C.; Challacombe, M.; Gill, P. M. W.; Johnson, B.; Chen, W.; Wong, M. W.; Andres, J. L.; Gonzalez, C.; Head-Gordon, M.; Replogle, E. S.; Pople, J. A., Gaussian Inc., Pittsburgh, PA, 1998.

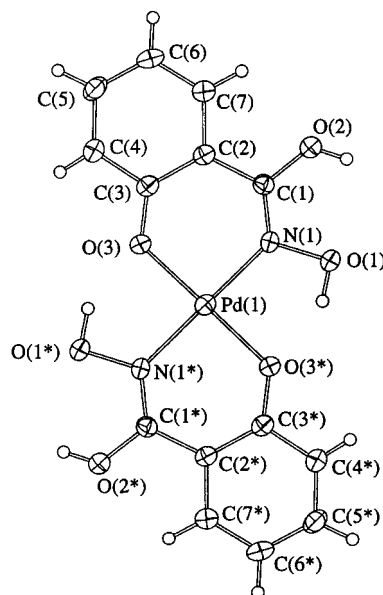
(30) Lee, C.; Yang, W.; Parr, R. G. *Phys. Rev. B* **1988**, *37*, 785–789.

(31) Becke, A. D. *Phys. Rev. A* **1988**, *38*, 3098–3100.

(32) Becke, A. D. *J. Chem. Phys.* **1993**, *98*, 5648–5652.

(33) Andrae, D.; Haeussermann, U.; Dolg, M.; Stoll, H.; Preuss, H. *Theor. Chim. Acta* **1990**, *77*, 123–141.

(34) Dunning, T. H.; Hay, P. J. In *Modern Theoretical Chemistry*; Schaefer, H. F., Ed.; Plenum: New York, 1976.

**Figure 2.** ORTEP representation of bis(salicylhydroxamato)palladium(II) (the asterisks indicate $-x$, $-y$, $-z$).

Results

Syntheses. A small number of palladium(II) complexes with hydroxamic acids have been reported previously, but no crystal structures have been published.²¹ The synthesis of bis(salicylhydroxamato)palladium(II) was relatively straightforward, and no adjustment of the pH of the reaction mixture was required to obtain the product.

Repeated attempts at synthesis of bis(salicylhydroxamato)platinum(II) via several methods resulted in reduction of the platinum(II) species despite ensuring reactions were undertaken in the dark to avoid this. The synthetic schemes used were analogous to those reported for the preparation of many bidentate oxygen donor ligands with platinum(II).³⁵ For example, a diaminedisolvantoplatinum(II) complex stirred with the hydroxamate in a number of solvents resulted in rapid reduction. Raising the pH of the solution to deprotonate the hydroxamic acid and promote coordination did not prove successful either. [Pt(sha-H)(PPh₃)₂] was readily synthesized, by reaction at pH 10–12 of *cis*-[PtCl₂(PPh₃)₂] and salicylhydroxamic acid.

Description of the Crystal Structures. An ORTEP²⁵ depiction of [Pd(sha)₂] is provided in Figure 2 and that of [Pt(sha-H)(PPh₃)₂] in Figure 3 with ellipsoids shown at the 30% level. Crystal structure data, selected bond lengths and selected bond angles for the complexes are presented in Tables 1–3.

The crystal structure of bis(salicylhydroxamato)palladium(II) revealed an unexpected binding mode in that the ligand is bound through the deprotonated nitrogen and phenolate oxygen [*N,O'*] donor atoms rather than through the oxygen atoms of the hydroxamic acid functional group [*O,O*]. As a result of coordination, the carbonyl oxygen atom is protonated, and the hydroxamate nitrogen and phenolate oxygen donor atoms are deprotonated, resulting in a uninegative

(35) Grunberg, A. A. *Helv. Chim. Acta* **1931**, *14*, 455–460.

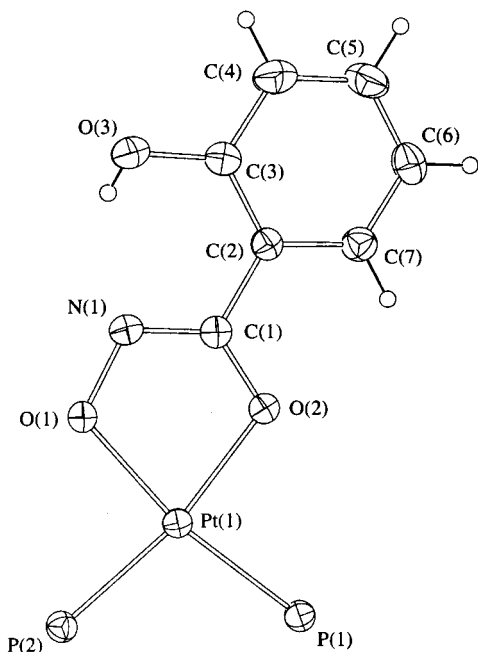


Figure 3. ORTEP representation of salicylhydroxamato-bis(triphenylphosphine)platinum(II) (phenyl rings omitted for clarity).

Table 2. Selected Bond Lengths (Å) and Angles (deg) for [Pd(sha)₂](DMF)₄^a

Pd(1)–O(3)	1.968(2)	C(2)–C(3)	1.419(4)
Pd(1)–N(1)	1.981(3)	C(2)–C(7)	1.397(5)
O(1)–N(1)	1.398(3)	C(3)–C(4)	1.418(4)
O(2)–C(1)	1.319(4)	C(4)–C(5)	1.364(5)
O(3)–C(3)	1.316(4)	C(5)–C(6)	1.381(5)
N(1)–C(1)	1.294(4)	C(6)–C(7)	1.379(5)
C(1)–C(2)	1.463(4)		
O(3)–Pd(1)–O(3*)	180.00	C(1)–C(2)–C(7)	117.2(3)
O(3)–Pd(1)–N(1)	92.2(1)	O(3)–C(3)–C(2)	125.9(3)
O(3)–Pd(1)–N(1*)	87.8(1)	O(3)–C(3)–C(4)	116.6(3)
N(1)–Pd(1)–N(1*)	180.00	C(1)–C(2)–C(3)	124.3(3)
Pd(1)–O(3)–C(3)	126.1(2)	C(2)–C(3)–C(4)	117.5(3)
Pd(1)–N(1)–O(1)	118.0(2)	C(3)–C(4)–C(5)	122.4(4)
Pd(1)–N(1)–C(1)	128.6(2)	C(4)–C(5)–C(6)	119.7(4)
O(1)–N(1)–C(1)	113.4(3)	C(5)–C(6)–C(7)	119.8(4)
O(2)–C(1)–N(1)	122.4(3)	C(2)–C(7)–C(6)	122.0(4)
O(2)–C(1)–C(2)	114.8(3)	C(3)–C(2)–C(7)	118.5(3)
N(1)–C(1)–C(2)	122.8(3)		

^a The asterisk indicates $-x, -y, -z$.

ligand and a neutral complex. The ligands are bound in a trans arrangement.

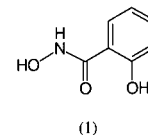
The deprotonated phenolato oxygen atom, O(3), is intramolecularly hydrogen bonded to the hydroxamate hydroxyl group of the opposite ligand. Two such hydrogen bonds are present per complex. Aside from the structural changes, previously reported bond lengths for the free ligand shaH can be used to gain insight into the nature of the ligand once bound to palladium(II).³⁶ The hydroxamate functional group bond lengths in the bound ligand are changed noticeably. The C(1)–O(2) (+0.026 Å) bond length is increased due to partial loss of its double bond character, and the C(1)–N(1) (–0.022 Å) and C(1)–C(2) (–0.026 Å) bonds are correspondingly shortened due to the delocalization of the carbonyl double bond. The N(1)–O(1) bond length would also be expected to be shortened due to the delocalized

Table 3. Selected Bond Lengths (Å) and Angles (deg) for [Pt(sha–H)(PPh₃)₂]

C(1)–N(1)	1.297(6)	C(5)–C(6)	1.363(10)
C(1)–O(2)	1.322(6)	C(6)–C(7)	1.387(8)
C(1)–C(2)	1.476(7)	N(1)–O(1)	1.398(6)
C(2)–C(7)	1.383(8)	O(1)–Pt(1)	2.045(3)
C(2)–C(3)	1.404(7)	O(2)–Pt(1)	2.072(3)
C(3)–O(3)	1.349(7)	P(1)–Pt(1)	2.2335(17)
C(3)–C(4)	1.388(9)	P(2)–Pt(1)	2.2062(13)
C(4)–C(5)	1.366(9)		
N(1)–C(1)–O(2)	124.0(5)	C(5)–C(6)–C(7)	119.7(6)
N(1)–C(1)–C(2)	118.1(5)	C(2)–C(7)–C(6)	121.0(5)
O(2)–C(1)–C(2)	117.9(4)	C(1)–N(1)–O(1)	114.7(4)
C(7)–C(2)–C(3)	118.7(5)	N(1)–O(1)–Pt(1)	112.2(3)
C(7)–C(2)–C(1)	119.6(4)	C(1)–O(2)–Pt(1)	109.6(3)
C(3)–C(2)–C(1)	121.7(5)	O(1)–Pt(1)–O(2)	79.21(13)
O(3)–C(3)–C(4)	118.9(5)	O(1)–Pt(1)–P(2)	90.14(10)
O(3)–C(3)–C(2)	121.9(5)	O(2)–Pt(1)–P(2)	169.10(10)
C(4)–C(3)–C(2)	119.2(5)	O(1)–Pt(1)–P(1)	169.12(10)
C(5)–C(4)–C(3)	120.9(6)	O(2)–Pt(1)–P(1)	89.99(10)
C(6)–C(5)–C(4)	120.5(6)	P(2)–Pt(1)–P(1)	100.59(5)

double bond, but it is marginally lengthened perhaps because of coordination of the nitrogen to palladium. There is also a shortening of the O(3)–C(3) (–0.039 Å) bond on coordination which is accompanied by lengthening of the adjacent C(3)–C(4) (+0.033 Å) and C(3)–C(2) (+0.018 Å) bonds. The metal–ligand bonds are relatively short, the Pd–O bond length being 1.968(2) Å and the Pd–N bond length 1.981(3) Å. These short bonds are presumably due to ionic contributions to the bonds; O(3) and N(1) are both deprotonated and carry negative charges. On the basis of the protonation state, the ligand is formally a hydroxamate, but the bond lengths are more consistent with the hydroximate form.

A thermal ellipsoid representation of the crystal structure of [Pt(sha–H)(PPh₃)₂] is shown in Figure 3. Unlike [Pd(sha)₂], the salicylhydroxamate ligand is observed to coordinate through both oxygen atoms of the hydroxamate functional group, with the phenolato oxygen remaining protonated. An unexpected feature is that the complex is neutral—indicating that the hydroxamate ligand is doubly deprotonated and hence is present in its hydroximate form. This is borne out by the difference in bond lengths from those in the free ligand: C(1)–N(1) –0.019, C(1)–O(2) +0.064, N(1)–O(1) +0.008. These observations are also in accord with those for the analogous complex [Pt(bha)(PPh₃)₂] (bha = benzohydroxamate) reported previously.³⁷ An intramolecular hydrogen bond between N(1) and O(3) is observed. This provides a degree of stabilization for the deprotonated N(1) and enforces coplanarity of the phenyl ring with respect to the hydroxamate functionality.



¹H NMR Solution Study. ¹H NMR was employed to investigate speciation of [PtCl₄]²⁻ and shaH in aqueous solution. A summary of the ¹H NMR spectra collected is shown in Table 4. Platinum(0) was noted to have formed in

(36) Larsen, I. K. *Acta Crystallogr.* **1978**, B34, 965–968.

(37) Bellon, P. L.; Cenini, S.; Demartin, F.; Manassero, M.; Pizzotti, M.; Porta, F. J. *Chem. Soc., Dalton Trans.* **1980**, 2060–2067.

Table 4. Summary of ^1H NMR Spectra Collected of Aqueous (D_2O) Solutions of $\text{K}_2[\text{PtCl}_4]$ and Salicylhydroxamate with Varying pH^a

pH	4 h	1 week	2 weeks
2	collected	collected	reduced
5	collected	reduced	reduced
13	collected	collected	reduced

^a When the solutions were noted to be reduced, spectra were not collected.

Table 5. Relative Energies of the Two Coordination Modes for Palladium(II) and Platinum(II) Modes (kJ mol^{-1}) Calculated Using the B3LYP/6-311G* Level of Theory

binding mode	[Pd(sha) ₂]	[Pt(sha) ₂]
[N,O]	0.0	0.0
[O,O]	81.55	219.64

a number of solutions after 1 week, despite storage in the dark at 5 °C. The ^1H NMR spectra of solutions showing evidence of solid platinum were not collected.

A typical ^1H NMR spectrum collected after 4 h following the preparation of the $\text{K}_2[\text{PtCl}_4]$ and shaH solution is provided in the Supporting Information. The spectra for all samples are similar, peaks due to the hydrogen atoms of the free ligand being shifted as a result of the large pH differences in solutions. Shifted ^1H peaks in the phenyl region (7–8 ppm) due to coordinated salicylhydroxamate are observed only on expansion of the region, the intensity of bound peaks being several orders of magnitude less than those of the free ligands. Proton signals for the amide, hydroxyl, and phenolato hydrogens in the free ligand were not present in the ^1H NMR spectra collected due to proton exchange with D_2O . There was no observable increase in the intensity of peaks assigned to the bound ligand after 1 week, and platinum(II) in all solutions was noted to be reduced by 2 weeks. As the intensities of the shifted species in the spectra listed in Table 4 were similar, they are not all displayed.

Computational Studies. The crystal structure of $[\text{Pd}(\text{sha})_2]$ revealed an $[\text{N},\text{O}']$ coordination mode, and subsequent ^1H NMR of the synthetic product revealed only one isomer was present. To determine whether the expected $[\text{O},\text{O}]$ isomer was viable, the relative energies of both isomers were determined using DFT. The bond lengths and angles of the optimized geometry are provided as Supporting Information. As an extension of this work, the relative energies of the $[\text{O},\text{O}]$ and $[\text{N},\text{O}']$ isomers of $[\text{Pt}(\text{sha})_2]$ were also examined. The results for both metal complexes are shown in Table 5. The $[\text{N},\text{O}']$ isomer of $[\text{Pd}(\text{sha})_2]$ was found to be substantially more stable by DFT, and this was the isomer which crystallized. Only one isomer was observed in the ^1H NMR spectrum of the product. The $[\text{N},\text{O}']$ isomer of $[\text{Pt}(\text{sha})_2]$ was also shown to be more stable than the $[\text{O},\text{O}]$ isomer, and to a greater extent than for the corresponding palladium(II) complexes.

Discussion

A number of hydroxamic acid complexes with transition metals have been reported in which the hydroxamate group has rearranged to a hydroximate group, similar to that found in the platinum and palladium complex crystal structures here. This occurs by deprotonation of the nitrogen and

**Figure 4.** Hydroxamic acid and hydroximate functional groups.

delocalization of the carbonyl double bond, as shown in Figure 4. While this can be promoted by basic conditions,³⁸ it has been seen to occur spontaneously in DMF and acetone without addition of base.^{39,40} However, in all reported instances, the hydroxamate group has remained coordinated to the transition-metal center via an $[\text{O},\text{O}]$ coordination mode, including an instance where a molybdenum(III) complex possessed both a hydroxamate and a hydroximate ligand.⁴⁰ In the instance of $[\text{Pd}(\text{sha})_2]$, the hydroxamate oxygen atoms play no part in the coordination. This coordination mode has not been previously described.

The ^1H NMR of platinum(II) with salicylhydroxamate confirmed the instability of the desired bis complex. The ^1H NMR displayed evidence of only one species, which corresponded to that of the free ligand. All bishydroxamate complexes with the platinum metals reported have been insoluble in H_2O , and as such it is unlikely that the bishydroxamateplatinum(II) species is present at equilibrium to a significant extent.^{21,41}

However, salicylhydroxamic acid is able to form stable complexes with platinum(II) when it adopts the hydroximate form. The successful synthesis and characterization of $[\text{Pt}(\text{sha}-\text{H})(\text{PPh}_3)_2]$ show that the hydroximate form of the ligand is apparently stabilized when soft ligands lie *trans* to it. This is also observed in the related complex $[\text{Pt}(\text{bha})(\text{PPh}_3)_2]$, other compounds synthesized in our laboratories with DMSO ligands, and a dinuclear Pt complex.⁴² Unless a means of stabilizing the hydroximate form is present, the likelihood of obtaining a platinum–hydroxamate complex appears low. The palladium complex also showed this preference for the hydroximate form, but in this case coordinated in the $[\text{N},\text{O}']$ binding mode, rather than the $[\text{O},\text{O}]$ binding mode.

Investigations of the coordination modes of bis complexes using DFT indicate that for both metals the $[\text{N},\text{O}']$ binding mode is far more stable than the $[\text{O},\text{O}]$ binding mode, as indicated in Table 5, as one would expect using HSAB rules. While the relative stabilities of the isomers of the platinum(II) complexes are indicated, the absolute stabilities cannot be determined by this method. The DFT energies alone prove insightful, however, in light of the experimentally observed instability of these complexes. While palladium(II) complexes with salicylhydroxamate ligands in an $[\text{N},\text{O}']$ mode, platinum(II) seems to be too soft (HSAB) to form a salicylhydroxamate coordination complex in either the $[\text{O},\text{O}]_2$ or $[\text{N},\text{O}']_2$ binding mode.

(38) Abu-Dari, K.; Barclay, S. J.; Riley, P. E.; Raymond, K. N. *Inorg. Chem.* **1983**, *22*, 3085–3089.

(39) Lah, M. S.; Pecoraro, V. L. *J. Am. Chem. Soc.* **1989**, *111*, 7258–7259.

(40) Lin, S. P.; Khan, M. A.; Nicholas, K. M. *Chem. Commun.* **1994**, 2425–2426.

(41) O'Brien, E. C.; Le Roy, S.; Levaillain, J.; Fitzgerald, D. J.; Nolan, K. B. *Inorg. Chim. Acta* **1997**, *266*, 117–120.

(42) Failes, T. W.; Hambley, T. W., to be submitted.

The molecular structure of $[\text{Pd}(\text{sha})_2]$ obtained from the DFT optimization shows some notable differences between experiment and theory. This was mainly manifest in the coordination sphere around the Pd atom where large distortions from square planar geometry are evident. This may be partially attributed to some distortions within the chelate ring of the sha ligand itself. The $\text{O}(3)\text{--Pd}(1)\text{--N}(1)$ angle calculated is somewhat closed (85.4°) compared to 92.2° observed in the crystal structure, whereas the angle $\text{O}(3)\text{--Pd}(1)\text{--N}(1^*)$ has a calculated value of 94.6° and an experimental value of 87.8° . The calculated Pd–N bond lengths of 1.99 Å are very close to the experimentally observed value of 1.98 Å; however, there is a distinct shortening of the Pd–O bond lengths in the calculated structure (1.88 Å vs 1.96 Å). The $\text{N}(1)\text{--C}(1)$ bond length (1.39 Å) remains longer than that determined experimentally (1.29 Å), and the $\text{O}(1)\text{--N}(1)\text{--C}(1)$ bond angle is closed by approximately 4° with respect to the experimental value. The $\text{O}(3)\text{--C}(3)$ bond length is only marginally overestimated from the observed value (1.33 Å vs 1.31 Å), with a calculated $\text{O}(3)\text{--C}(3)\text{--C}(2)$ angle of 124.0° (125.9° , experimental). The remaining geometrical parameters show very good agreement between the optimized structure and what is observed experimentally.

As a carrier for therapeutic MMP inhibitors such as marimastat and batimastat, palladium(II) and platinum(II) complexes do not appear promising. $[\text{Pd}(\text{sha})_2]$ is insoluble

in aqueous solution at physiological pH, and the hydroxamate functional group was not coordinated and protected. Palladium(II) complexes are also labile relative to platinum(II) complexes, and this lability has hampered attempts to use palladium(II) complexes as cisplatin-like antitumor agents as they are aquated and react rapidly with biological media in vivo.⁴³ If more inert platinum(II) complexes with therapeutic MMP inhibitors were synthesized, it is likely, as for palladium(II), that the inhibitors would coordinate through other donors (S or N) on the drug preferentially to the hydroxamate moiety. Transition-metal hydroxamate complexes with two nonleaving donors (e.g., amines) may have improved solubility and provide an effective carrier complex.

Acknowledgment. We thank the Australian Research Council and the University of Sydney Cancer Research Fund for financial support.

Supporting Information Available: Figure showing an expansion of the phenyl region of the ^1H NMR spectrum of $[\text{PtCl}_4]^{2-}$ and salicylhydroxamic acid and an enlargement of the spectrum showing little or no complexation at equilibrium, a table giving bond lengths and angles for $[\text{Pd}(\text{sha})_2]$, and crystallographic data in CIF format. This material is available free of charge via the Internet at <http://pubs.acs.org>.

IC010760Q

(43) Hambley, T. W. *Coord. Chem. Rev.* **1997**, *166*, 181–223.